ARTICLES

Semiempirical Pseudopotential Calculation of Electronic States of CdSe Quantum Rods

Jiangtao Hu,[†,‡] Lin-wang Wang,[§] Liang-shi Li,[†,‡] Weidong Yang,[†,‡] and A. Paul Alivisatos*[,†,‡]

Department of Chemistry, University of California at Berkeley, Berkeley, California 94720, Materials Science Division, Lawrence Berkeley National Laboratory, 1 Cyclotron Road, Berkeley, California 94720, National Research Scientific Computing Center, Lawrence Berkeley National Laboratory, 1 Cyclotron Road, Berkeley, California 94720

Received: August 17, 2001; In Final Form: December 11, 2001

The dependence of electronic states on the length and diameter of CdSe quantum rods is investigated using semiempirical pseudopotential calculations. Energy levels cross as the aspect ratio increases due to their different dependence on length. The crossover between the highest occupied levels leads to a transition from plane-polarized to linearly polarized light emission at aspect ratio ca. 1.3. Further increasing aspect ratio results in levels with similar symmetry converging and forming "bands". This calculation demonstrates the transition of electronic structure from zero-dimensional quantum dots to one-dimensional quantum wires.

1. Introduction

Colloidal CdSe quantum dots (QD) have received intensive experimental and theoretical study during the past decade due to their rich phenomena associated with quantum confinement and due to their ready availability.[1,2] In the case of spherically shaped CdSe colloidal quantum dots, their syntheses have been so well developed that they have become a model system for studying quantum size effects.[3,4] Experimentally, their band gap and oscillator strength can be tuned by variation of the diameters and many novel phenomena, such as "blinking"[5] and spectral diffusion,[6] are observed. Theoretical studies of the electronic structure by first using effective mass approximation models,[7,8] and more recently empirical pseudopotential methods[9] are able to explain many of the experimentally observed size effects.

The shape effect, on the other hand, has received much less attention not because it is less interesting, but mainly because it was not until recently that a controllable synthesis approach for varying the shape of colloidal quantum dots became available.[10,11] Because CdSe has a hexagonal crystal structure, elongation along crystallographic *c*-axis produces many pronounced changes in electronic structure. Novel behaviors can be expected when shape is controlled. Recent observations of the unique properties of CdSe quantum rods, e.g., nonmonotonic change of global Stokes shift with aspect ratio and highly linearly polarized photoluminescence emission from even slightly elongated quantum rods[10,12] are just the beginning of discovering the role of shape in these systems. At this stage, a detailed theoretical study on the electronic structures of CdSe quantum rods is thus important and timely.

2. Calculation

The electronic structure of CdSe quantum rods is calculated using the semiempirical pseudopotential method.[13] On the bases of the ab initio local density approximation (LDA) calculations on bulk CdSe, approximated screened atomic spherical potentials that reproduce the bulk LDA potential for Cd and Se atoms are developed. Small modifications are made to the screened atomic potentials to correct the LDA band gap errors, and to fit to the bulk CdSe band structure. The resulting semiempirical pseudopotentials $v^{\alpha}(r)$ [α stands for atomic types, Cd or Se] are used to construct the single particle Hamiltonian and the corresponding Schrödinger equation:

$$\left\{-\frac{1}{2}\nabla^2 + \sum_{\alpha,R} v^{\alpha}(|r-R|) + \hat{V}_{\text{nonlocal}}(r)\right\}\psi_i(r) = \epsilon_i\psi_i(r)$$

where R's are the atomic positions, and $\hat{V}_{\text{nonlocal}}(r)$ the nonlocal part of the pseudopotential, which is the same as that in the LDA ab initio pseudopotentials. The wave functions $\{\psi_i(r)\}$ are expressed in a planewave basis set, using a cutoff of 6.8 Rydberg for the planewave kinetic energy. Spin−orbit coupling is included in the nonlocal potential $\hat{V}_{\text{nonlocal}}(r)$. As a result, the wave functions $\{\psi_i(r)\}$ are spinors with spin up and spin down components.

A rod shape is generated from the bulk wurtzite CdSe with the long axis along the crystallographic *c*-axis. To change the aspect ratio of the rod, we start from a spherical dot with the desired diameter and insert a cylindrical segment along the *c*-axis. We have removed surface Cd and Se atoms with only one bond connected to the rest of the rod. As a result, the numbers of Cd and Se atoms may not be the same. However, as we are not doing total energy calculations, such a slight nonstoichiometry is not a problem in our calculation. The surface Cd and Se atoms are passivated using different hypothetical ligand potentials. This is in part to simulate the experimental situation of surfactant passivation, and in practice to remove surface dangling bond states from the band gap. The detail of this passivation is described in ref 9. In terms of calculation, this is to add a few additional atomic types α and their

[†] Department of Chemistry.
[‡] Materials Science Division.
[§] National Research Scientific Computing Center.

10.1021/jp013204q CCC: $22.00
Published on Web 02/12/2002

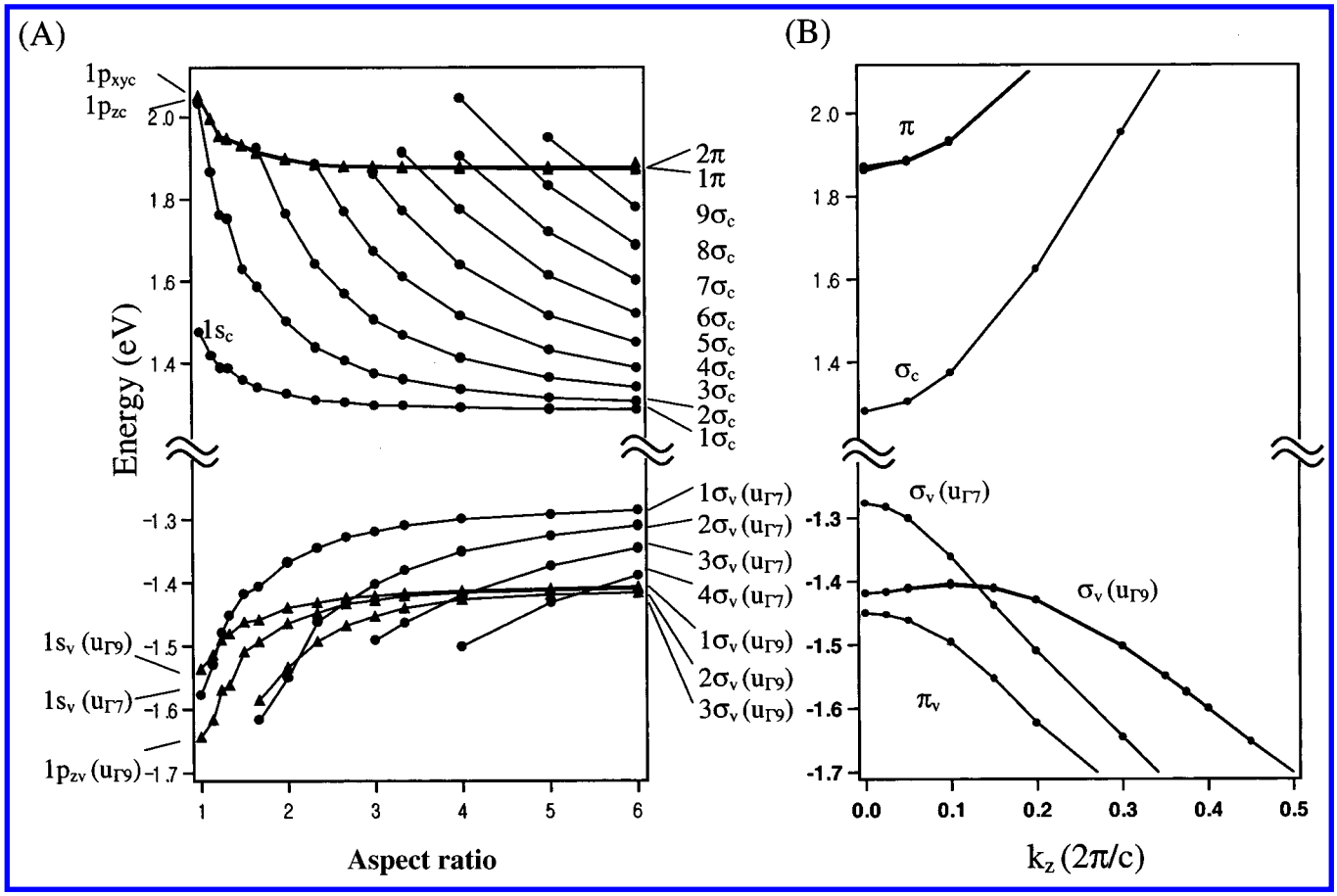

Figure 1. (A) The evolution of energy levels of the band edge levels versus aspect ratio for 2.0 nm diameter quantum rods.The marks are calculated results and solid lines connect the same levels between different aspect ratios. For unoccupied levels, closed circles are the levels with σ-type envelope function in the xy-plane and closed triangles are the levels with π-type envelope function in the xy-plane. For occupied levels, closed circles are the levels consist of mainly Se $4p_z$ atomic orbitals and closed triangles the levels consist of mainly $4p_{x,y}$ atomic orbitals. (B) The band structures of 2.0 nm diameter quantum wires. The marks are calculated results and solid lines simply connect the calculated results.

corresponding passivation potentials $v^{\alpha}(r)$ in the Schrödinger equation above.

The Schrödinger equation is solved for eigenstates $\{\psi_i(r)\}$ near the band edge. This is done with the folded spectrum method (FSM).[14] Only a few levels near the band edge are solved independently of the size of the rod. As a result, the method scales linearly to the size of the system. A parallel program (Escan) is developed based on FSM. It uses a parallel FFT, and a real space implementation of the nonlocal potential in the above equation.[15] The current calculations are carried out using the Cray T3E parallel computer in National Energy Research Scientific Computing Center (NERSC).

The above approach has been used extensively to study the electronic structures of CdSe quantum dots. These include band gap vs the dot size, optical absorption spectra, higher excited states, Coulomb and exchange interactions, multiexciton fine structures, etc. Here we apply it to CdSe quantum rods, especially to study the changes of the electronic structures as the aspect ratio of the rods changes.

3. Results and Discussion

We have calculated energy levels and electron density distribution for the highest occupied molecular orbitals (HOMO) and the lowest unoccupied molecular orbitals (LUMO), and the oscillator strength of the transitions between them for CdSe quantum rods with diameters of 2.0, 3.0, and 3.8 nm, respectively. For 2.0 nm diameter quantum rods, more than six HOMO levels and six LUMO levels are calculated for aspect ratio ranging from 1.0 to 6.0. The band structures of an infinitely long 2.0 nm diameter nanowire are also calculated. Because the number of atoms increases quickly with increasing diameter and aspect ratio, as shown in Table 1, fewer energy levels are calculated for 3.0 and 3.8 nm diameter quantum rods with a smaller range of aspect ratio. The results for the thicker quantum rods qualitatively agree with those for the 2.0 nm wide rods, therefore our description and discussion of the results are mainly based on the calculation for 2.0 nm diameter ones, which we believe are representative for quantum rods with diameter in the quantum confinement regime.

TABLE 1: Total Number of Cd and Se Atoms vs the Size of Quantum Rods[a]

diameter (nm)	length (nm)	aspect ratio	atom number
2.0	2.0	1.0	164
2.0	6.0	3.0	644
2.0	12.0	6.0	1,367
3.0	3.0	1.0	470
3.0	7.3	2.4	1,490
3.0	14.4	4.4	3,190
3.8	3.8	1.0	1,055
3.8	5.3	1.4	1,623
3.8	8.0	2.1	2,759

[a] The largest structure we have calculated contains 3190 atoms, which requires a computing time of 2.3 hours on a Cray T3D machine using 64 processors.

Figure 1A summarizes the evolution of energy levels of the energy levels vs aspect ratio for 2.0 nm diameter quantum rods. Levels are identified by the symmetry of electron density

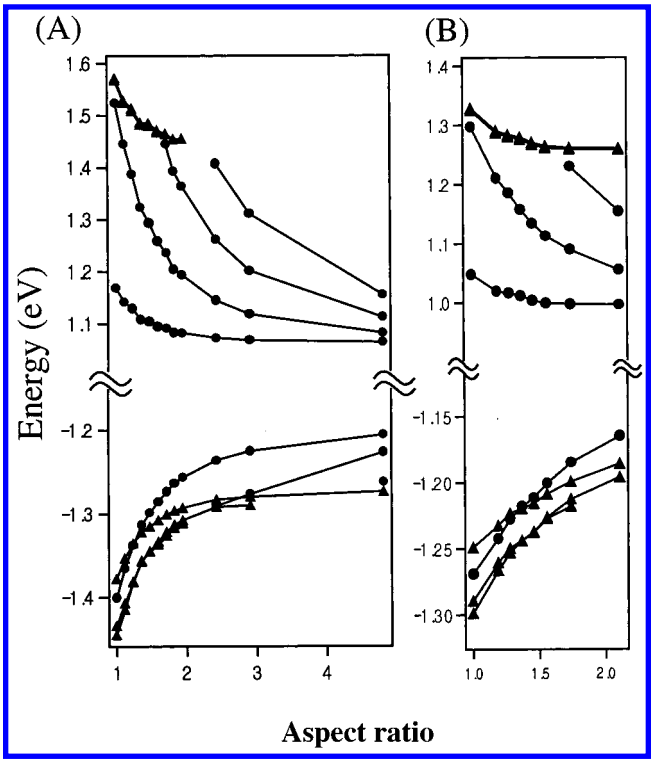

Figure 2. The change of energy levels of the band edge levels versus aspect ratio for (A) 3.0 nm and (B) 3.8 nm diameter quantum rods.The marks and lines have the same meaning as that in Figure 1A.

distribution (see Figure 4). The energy levels with the same symmetry for rods with different aspect ratio are connected with solid lines. Several observations can be made from this figure. First, the energy of the electronic states decreases with increasing aspect ratio, as expected from quantum confinement. Qualitatively, in CdSe the HOMOs originate from Se 4p atomic orbitals and LUMOs from Cd 5s atomic orbitals. Excited electronic states arise when an electron is excited from an occupied Se 4p orbital to an empty Cd 5s orbital. This excitation is distributed throughout many unit cells and its energy is strongly dependent on the size of the crystal. Second, some energy levels depend on length much more than others, and level crossings occur. Increasing aspect ratio only reduces confinement along the *z*-axis and therefore has greater effect on those levels more sensitive to confinement in the *z*-direction. Third, the levels are converging into several distinct "bands" with increasing aspect ratio. This can be attributed to the transition from a zero-dimensional (0D) to a one-dimensional (1D) system, where a continuous band forms along the *z*-direction. To further illustrate this transition, we also calculated the energy bands of a 2.0 nm diameter quantum wire (Figure 1B). For the quantum wire, the lowest conduction bands are σ_v and π_v. They both originate with Cd 5s orbitals and respectively have σ- and π- type envelope functions in the *xy*-plane. The π_c bands are doubly degenerate. The two highest valence bands are from Se 4p orbitals. They are either dominated by the p_z orbitals, denoted as $u_{\Gamma 7}$, or the $p_{x,y}$ orbitals, denoted $u_{\Gamma 9}$. The envelope functions can also be either σ or π symmetry. It is worth noting that while other bands have extrema at $k_z = 0$, the maximum for σ_v ($u_{\Gamma 9}$) band is at $k_z \sim 0.3\pi/c$. Figure 1 clearly shows that the converging energy levels of quantum rods are aligned with energy band at $k_z = 0$ of the nanowires, with the exception of σ_v. The relationship between the individual levels in Figure 1A and the continuous band in Figure 1B will be discussed in more details below.

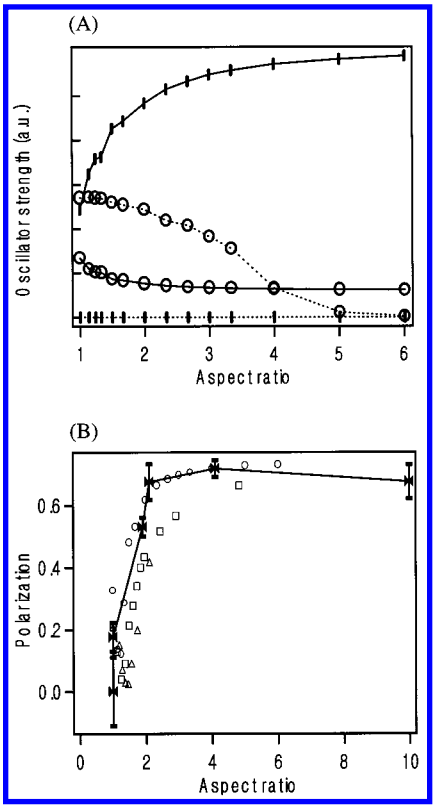

Figure 3. (A) Oscillator strength of the transition between the lowest unoccupied level and the two highest occupied levels (level-1 and level-2). Solid line is for level-2 and dotted line is for level-1. Vertical bars are the *z* component of each transition and open circles are the *x* component of each transition. The *z* component for level-1 is zero. (B) Polarization factor versus aspect ratio. Solid marks with error bars are from experiments and open marks are from the calculations for 2.0 nm (circle), 3.0 nm (square), and 3.8 nm (triangle) diameter quantum rods.

We also calculated the HOMOs and LUMOs of quantum rods with diameters of 3.0 and 3.8 nm (Figure 2). The aspect ratio ranges from 1.0 to 4.8 and from 1.0 to 2.1 for these two diameters, respectively. Qualitatively, the changes of energy levels with aspect ratio of the two thicker quantum rods are the same as that of 2.0 nm thick quantum rods. The main effect of increasing the diameter is to decrease the spacing between energy levels.

The level crossing between the two highest occupied levels is particularly important because generally it is the relaxation of the electron from the lowest unoccupied level to the highest occupied level that gives off luminescence. This crossing occurs at the aspect ratio of 1.25, 1.25, and 1.36 for 2.0, 3.0, and 3.8 nm wide quantum rods, respectively (Figure 1A and Figure 2). These two levels both originate from Se 4p atomic orbitals but one of them mainly consists of $4p_{x,y}$ orbitals and the other mainly $4p_z$ orbitals (Figure 4B). For spherical quantum dots, the electronic levels with mainly $p_{x,y}$ components (level-1 hereafter) have slightly higher energy than levels with mainly p_z component (level-2 hereafter) due to the anisotropic structure of Wurtzite CdSe.[7] While the oscillator strength of the transition from LUMO to level-1 has only *x* and *y* components and that of the transition to level-2 is dominated by *z* component, the overall oscillator strengths are almost the same for the two levels because the LUMOs are from Cd 5s orbitals (Figure 3A). The energy of these two levels both increase with aspect ratio, but with a larger rate for level-2 because it has greater translational momentum projection onto the *c*-axis (*z*-axis) of the crystal compared to level-1 and is therefore more sensitive to the length

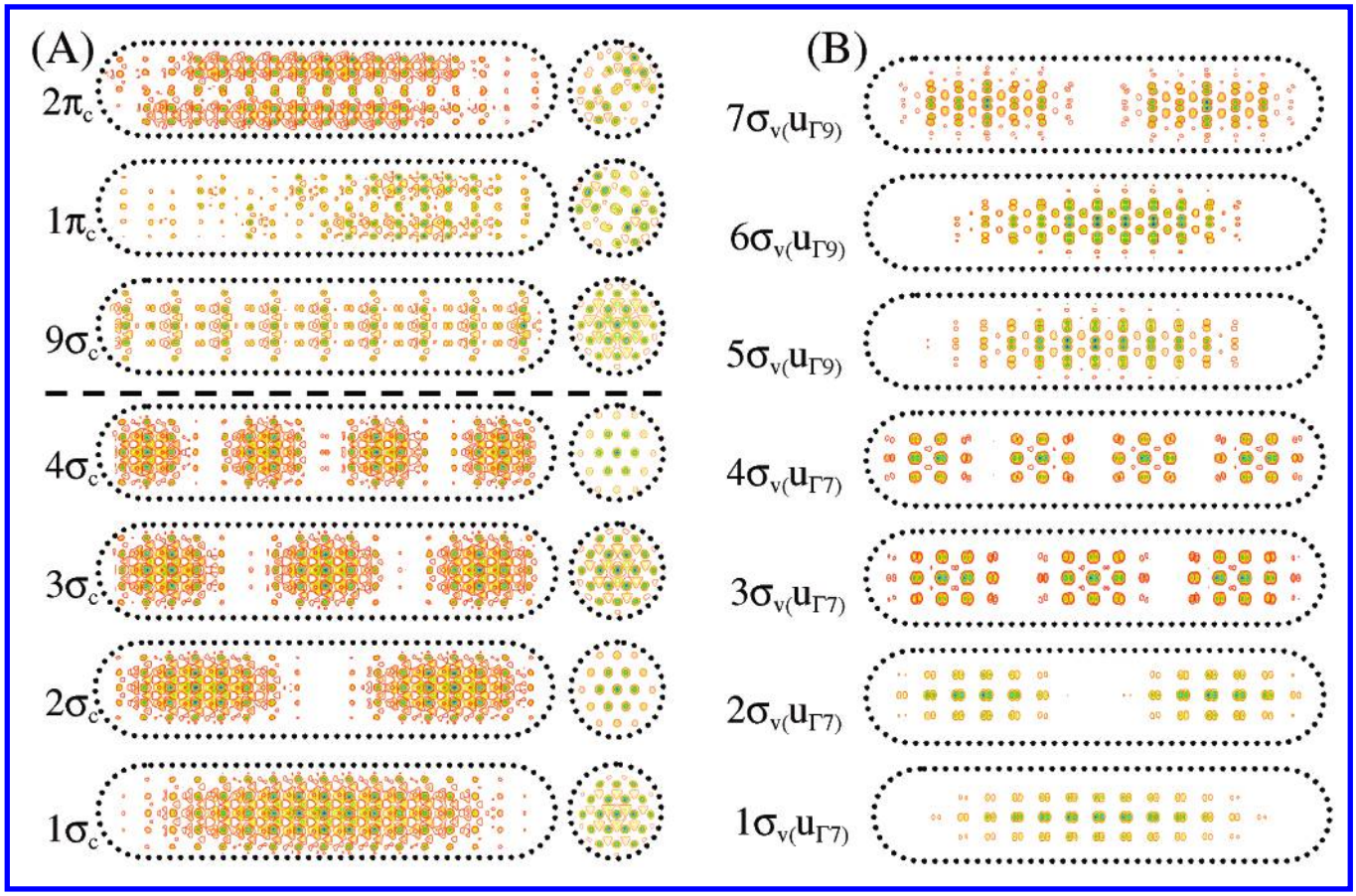

Figure 4. Electron density distribution of (A) LUMOs and (B) HOMOs in the plane along the *z*-axis and in the *xy*-plane for 2.0 nm diameter quantum rods with an aspect ratio of 6. (A) From top to bottom, the seven levels are the 1st−4th and 9th−11th lowest unoccupied levels in Figure 1A with an aspect ratio of 6. The atomic orbitals in the graphs are Cd 5s orbitals. The envelope functions for the first five graphs are σ-type in the xy-plane and contain 0−3, and 8 nodes along the *z*-axis. The envelope function for the last two graphs are π-type in the *xy*-plane and contain 0 node along the *z*-axis. These two levels are degenerated. (B) From top to bottom, the levels are the seven highest occupied levels in Figure 1A at the aspect ratio 6. In the first four graphs the atomic orbitals are mainly Se $4p_z$ orbitals and the envelope functions contain 0−3 nodes along the *z*-axis; in the last three graphs the atomic orbitals are Se $4p_x$ and p_y orbitals and the envelope functions are the mixture of the components containing 0, 1, 2, 3 ..., nodes along the *z*-axis. The envelope functions are σ-type in the *xy*-plane for all the levels.

of the quantum rods. Subsequently, these two levels exchange position at an aspect ratio greater than ca. 1.3 (i.e., 1.25 for 2.0 and 3.0 nm diameter and 1.36 for 3.8 nm diameter quantum rods) (Figure 1A and Figure 2). Furthermore, the overall oscillator strength of level-2 and the percentage of p_z component in level-2 both increase with aspect ratio (Figure 3A). This level crossing between the two HOMOs therefore results in a sharp transition from plane-polarized emission inside the *xy*-plane to highly linearly polarized emission along *z*-direction when the shape of the quantum dots change from spherical to slightly elongated. It has been experimentally demonstrated that spherical quantum dots emit light with polarization randomly distributed between zero and 100% at low temperature.[16] At room temperature, however, the emission of nearly spherical quantum dots will appear as only slightly polarized because the energy difference between the two excited levels is small compared to room temperature and the orientation of the quantum dots is random (open marks in Figure 3B). Experimental result obtained at room temperature by using single-dot luminescence spectroscopy is in excellent agreement with this theoretical prediction.[12] A sharp transition from nonpolarized emission to ca. 70% polarized emission occurs when aspect ratio of the quantum rods increases from 1.0 to 2.0 and then the percentage of polarization remains almost constant afterward (filled marks and line in Figure 3B). In the experiment, the diameters of quantum rods studied range from 3.0 to 3.5 nm, and the polarization for 2:1 quantum rods from 40% to 90% with an average of ca. 65%. Note that the degree of polarization in the light emission form the rods depends on how large the level spacing is compared to the thermal energy. Thus, the degree of polarization observed at room temperature can be reduced in dots of larger diameter, because all the energy levels start to converge, and there is thermal averaging. The highest degree of polarization will be observed in rods of smaller diameter, around 2.0 nm.

Besides the crossover between the two HOMOs, more crossovers occur both between unoccupied levels and between occupied levels. The unoccupied levels can be categorized into two groups, in which the energy of one (filled circles in Figure 1A) decreases much faster with aspect ratio than that of the other (filled triangles). These two groups of energy levels form two distinct "bands" at large aspect ratio. Since the LUMOs are formed from the nondegenerate Cd 5s atomic orbitals, the difference between these levels is in the envelope functions, which are determined by the shape of the nanocrystals. At an aspect ratio of 1.0, the quantum dots have spherical symmetry, therefore the envelop functions can be denoted as $1s_c$, $1p_{xc}$, $1p_{yc}$, $1p_{zc}$, etc. (Figure 1A), where subscript c stands for conduction level. Increasing the aspect ratio breaks the spherical symmetry and the symmetry of the envelope functions changes accordingly. Drawings of the distributions of electron density at an aspect ratio of 6.0 for these levels show that the electron density of the lowest unoccupied levels have σ-like distribution in the

xy-plane and no node along the *z*-axis (Figure 4A). The levels converging to it (filled circles in Figure 1A) all have σ-like distribution in the *xy*-plane but more than one node along the *z*-axis. The other group of energy levels (filled triangles in Figure 1A) has π-like distribution in the xy-plane. It is worth pointing out that, in principle, n_z and l_z are only approximately good quantum numbers in a quantum rod with finite length because of the mixing of the wave functions along the *z*- and *r*-directions. They become good quantum numbers only when the quantum rod is infinitely long, namely a 1D system (quantum wires), and spin−orbital coupling is not considered. However, the drawings show that at an aspect ratio of 6.0, it is a convenient and good approximation to use n_z and l_z to describe the envelope functions for the unoccupied levels. On the basis of the symmetry of the envelope functions, we denote the levels as $n\sigma_c$, $n\pi_c$, etc. (Figure 3A), where n is the number of levels counting from the LOMO, and σ and π denote the symmetry in the *xy*-plane. Here n coincides with n_z, the quantum number along *z*-direction. Both $1\sigma_c$ (the lowest unoccupied level) and $1\pi_c$ levels have no node along the *z*-direction. They are least sensitive to the length and quickly become flat after the initial drop in energy. Levels with more nodes along the *z*-axis are more sensitive to length and have larger energy drop with increasing aspect ratio. In other words, the energy separation between the $n = m$ and $n = m + 1$ levels decreases with aspect ratio. When the quantum rods become infinitely long, as in the case of quantum wires, $\{n\sigma_c\}$ and $\{n\pi_c\}$ levels form continuous bands, respectively. Due to the cylindrical symmetry of the quantum wires, the energy bands can be simply denoted as σ_c, π_c, δ_c, etc. (Figure 1B). Thus, we have established the correlation diagram between the individual levels in spherical quantum dots, the individual levels in quantum rods, and the continuous energy bands in quantum wires for the conduction levels and bands.

The situation for occupied levels is similar but slightly more complicated because they are formed from Se 4p orbitals. The levels consisting of predominantly $4p_z$ orbitals are not degenerate with those mainly containing $4p_x$, $4p_y$ orbitals and have stronger dependence on the confinement along the *z*-direction. To count for this contribution from the atomic orbitals, new symbols are included to label the levels. To be consistent with literature, $u_{\Gamma 9}$ is used for the levels with predominantly $p_{x,y}$ orbitals and $u_{\Gamma 7}$ for the levels with mainly p_z orbitals. The occupied levels of spherical quantum dots thus are labeled as $1s_v$ ($u_{\Gamma 9}$), $1s_v$ ($u_{\Gamma 7}$), $1p_{zv}$ ($u_{\Gamma 9}$), etc., and the levels of quantum rods with aspect ratio of 6 are labeled as $n\sigma_v$ ($u_{\Gamma 7}$), $n\sigma_v$ ($u_{\Gamma 9}$), etc. (Figure 1A). As aspect ratio increases to infinity, the $\{n\sigma_v (u_{\Gamma 7})\}$ levels converge into one band σ_v ($u_{\Gamma 7}$) and the $\{n\sigma_v (u_{\Gamma 9})\}$ levels converge into another band σ_v ($u_{\Gamma 9}$) (Figure 1B). While the envelope functions of $n\sigma_v$ ($u_{\Gamma 7}$) can still be conveniently identified with n_z (n coincident with n_z for highest occupied levels), the situation is more complicated for the $n\sigma_v$ ($u_{\Gamma 9}$) levels. This complication arises because the confinement energy due to the *z*-direction envelope of $p_{x,y}$ orbitals is so small—only a few meV when aspect ratio is larger than 4 (Figure 1A)—that the energy levels intermix with each other for different n_z's. In this case, these levels cannot be simply assigned to a single value of n_z. For example, detailed analysis shows that the lowest level consisting of $p_{x,y}$ components at aspect ratio of 6 is a mixture of $n_z = 1$, 2, 3, 4, etc. (Figure 4B). Here the even and odd n_z mix together since there is no exact inversion symmetry in the *z*-direction. The domination of higher n_z instead of the lowest $n_z = 0$ in the quantum rod state is corroborated with the energy dispersion of the corresponding state in the quantum wire shown in Figure 1B. The band energy of $\sigma_v(u_{\Gamma 9})$ has a maximum at finite k_z ($\sim 0.152\pi/c$) point, instead of at $k_z = 0$. The mixing of different n_z components in these levels is also reflected in the oscillator strength. In Figure 3A, the oscillator strength of level-1 drops quickly when aspect ratio larger than 3.3. It is because when aspect the ratio is larger than 3.3, this level is no longer primarily an $n_z = 1$ level, but becomes dominated by $n_z = 2$ level due to the coupling. If we sum over the oscillator strengths over the few energetically close levels consisting of $p_{x,y}$ components, the curve becomes smoother.

The major difference between 0-dimensional (0D) and 1D systems in the electronic structures is that 0D systems have discrete electronic levels while in 1D systems the levels different only in k_z (n_z) form continuous bands. In practice, however, all the structures here have finite length. When the "intraband" separations are small compared to thermal energy at the temperature of study, the bands can be regarded as "continuous". Our calculations of the electronic structures of CdSe quantum rods thus demonstrate the band formation as the system evolves from 0D to 1D. The 'bands' within a fixed range of spectrum close to the HOMO−LUMO gap (e.g., the ones that we have calculated) are experimentally most interesting. At an aspect ratio of 6 for 2.0 nm diameter quantum rods, the largest "intraband" separation, which occurs at the center of $\{n\sigma_c\}$ 'band' of the LUMOs, is on the order of 100 meV, much larger than thermal energy at room temperature, so this structure should still be considered as a 0D quantum dot even at room temperature. If the aspect ratio is two times larger (i.e., 12), the number of n_z will be 2 times larger as well and the "intraband" separation will be about 4 times smaller.[17] The "intraband" separation, especially at the edge of the "band", would be small compared to room temperature thermal fluctuation, and the structure can then be regarded as a 1D system. This conclusion has significant meaning because using current techniques CdSe quantum rods with length of 100 nm can be readily made. More versatile nanoscale electronic and optical devices that combine the advantages of 0D and 1D systems can potentially be made by using CdSe quantum rods as building blocks.

4. Summary

We have calculated the electronic energy levels of CdSe quantum rods with various diameters and aspect ratios using semiempirical pseudopotential calculations. In particular, the dependence of electronic states upon aspect ratio was investigated by examining the band edge energy levels of quantum rods with 2.0 nm diameter and aspect ratio ranging from 2.0 to 6.0. When aspect ratio increases, energy level crossing occurs for both HOMO and LUMO levels because some levels depend on length much more than others. For HOMO levels, the levels consisting of more Se $4p_z$ component are more strongly dependent on length than those consisting of mainly Se $4p_{x,y}$ components. The crossover between the two levels at an aspect ratio of $\sim$1.3 leads to nearly linearly polarized emission from even slightly elongated quantum rods. Furthermore, with the increasing length, the levels with the same symmetry of envelope functions but different in n_z converge into semicontinuous bands. By comparing with the band structure of nanowires with a diameter of 2.0 nm, it is shown that this convergence of energy levels is a signature of the transition from a 0-dimensional to a 1-dimensional nanostructure.

Acknowledgment. This work is supported by the Director, Office of Energy Research, Office of Science, and Division of Materials Sciences, of the U. S. Department of Energy (DOE)

under contract DE-AC03-76SF00098, by the National Institute of Health National Center for Research Resources grant 1 R01 RR-14891-01 under the same DOE contract number, and by Department of Defense Advanced Research Projects Agency (DARPA) under grant ONR N00014-99-1-0728. L-W. W. is supported by the Director, Office of Science, Division of Mathematical, Information, and Computational Science of DOE under contract DE-AC03-76SF00098. This research used resources of the National Energy Research Scientific Computing Center, which is supported by the Office of Science of DOE.

References and Notes

(1) Alivisatos, A. P. *Science* **1996**, *271*, 933.
(2) Brus, L. E. *Appl. Phys. A* **1991**, *53*, 465.
(3) Murray, C. B.; Norris, D. J.; Bawendi, M. G. *J. Am. Chem. Soc.* **1993**, *115*, 8706.
(4) Peng, X. G.; Wichham, J.; Alivisatos, A. P. *J. Am. Chem. Soc.* **1998**, *120*, 5343.
(5) Mimal, M.; et al. *Nature* **1996**, *383*, 802.
(6) Empedocles, S. A.; Bawendi, M. G. *Science* **1997**, *278*, 2114.
(7) Efros, Al. *Phys. Rev. B* **1992**, *46*, 7448.
(8) Efros, Al.; et al. *Phys. Rev. B* **1996**, *54*, 4843.
(9) Wang, L. W.; Zunger, A. *Phys. Rev. B* **1996**, *53*, 9579.
(10) Peng, X.; et al. *Nature* **2000**, *404*, 59.
(11) Manna, L.; Scher, E. C.; Alivisatos, A. P. *J. Am. Chem. Soc.* **2000**, *122*, 12700.
(12) Hu, J.; et al. *Science* **2001**, *292*, 2060.
(13) Wang, L. W.; Zunger, A. *Phys. Rev. B* **1995**, *51*, 17398.
(14) Wang, L. W.; Zunger, A. *J. Chem. Phys.* **1994**, 100, 2394.
(15) Canning, A.; Wang, L. W.; Williamson, A.; Zunger, A. *J. Comput. Phys.* **2000**, *160*, 29.
(16) Empedocles, S. A.; Neuhauser, R.; Bawendi, M. G. *Nature* **1999**, *399*, 126.
(17) The intraband separation between $n_z = 0$ and 1 scales as the inverse square of the aspect ratio and between $n_z = n_{z,max}$ and $n_{z,max} - 1$ scale as the inverse of the aspect ratio.